Numerical modeling of fiber lasers with long and ultra-long ring cavity

I.A. Yarutkina,[1,2,*] **O.V. Shtyrina,**[1,2] **M.P. Fedoruk,**[1,2] **and S.K. Turitsyn**[3]

[1] *Institute of Computational Technologies, Siberian Branch of the Russian Academy of Sciences, 6 Ac. Lavrentjev Avenue, Novosibirsk, 630090, Russia*
[2] *Novosibirsk State University, 2 Pirogova Street, Novosibirsk, 630090, Russia*
[3] *Aston Institute of Photonic Technologies, School of Engineering and Applied Science, Aston University, Birmingham, B4 7ET, UK*

[*] *i.yarutkina@gmail.com*

Abstract: We highlight two important aspects related to a mathematical modeling of pulsed fiber lasers with long and ultra-long ring cavity – impact of an initial noise and a cavity length on generation of single optical pulses. Using as an example a simple scalar model of a ring fiber laser that describes the radiation build-up from noise and the following intra-cavity pulse dynamics during a round trip we study dependence of generated pulse characteristics on the resonator length in the range from 30 m up to 2 km.

© 2013 Optical Society of America

OCIS codes: (140.3510) Fiber laser; (140.3560) Ring laser; (140.4050) Mode-locked lasers.

References and links

1. A. E. Siegman, *Lasers*, (University Science Books, 1986).
2. S. Kobtsev, S. Kukarin, and Y. Fedotov, "Ultra-low repetition rate mode-locked fiber laser with high-energy pulses," Opt. Express **16,** 21936–21941 (2008).
3. S. Kobtsev, S. Kukarin, S. Smirnov, A.I. Latkin, and S. Turitsyn, CLEO/Europe, CJ8 4, 2009.
4. S. Kobtsev, S. Kukarin, S. Smirnov, S.K. Turitsyn, and A. Latkin, "Generation of double-scale femto/pico-second optical lumps in mode-locked fiber lasers," Opt. Express **17,** 20707 (2009).
5. E.J.R. Kelleher, J.C. Travers, E.P. Ippen, Z. Sun, A.C. Ferrari, S.V. Popov, and J.R. Taylor, "Generation and direct measurement of giant chirp in a passively mode-locked laser," Opt. Lett. **34,** 3526–3528 (2009).
6. L. Chen, M. Zhang, C. Zhou, Y. Cai, L. Ren, and Z. Zhang, "Ultra-low repetition rate linear-cavity erbium-doped fibre laser modelocked with semiconductor saturable absorber mirror," Electron. Lett. **45,** 731 (2009).
7. B.N. Nyushkov, V.I. Denisov, S.M. Kobtsev, V.S. Pivtsov, N.A. Kolyada, A.V. Ivanenko, and S.K. Turitsyn, "Generation of 1.7-microJ pulses at 1.55 micrometer by a self-modelocked all-fiber laser with a kilometers-long linear-ring cavity," Laser Phys. Lett. 1–5 (2010).
8. B.N. Nyushkov, A.V. Ivanenko, S.M. Kobtsev, S.K. Turitsyn, C. Mou, L. Zhang, V.I. Denisov, and V.S. Pivtsov, "Gamma-shaped long-cavity normal-dispersion mode-locked Er-fiber laser for sub-nanosecond high-energy pulsed generation," Laser Phys. Lett. **9**(1), 56–67 (2012).
9. A. Ivanenko, S. Turitsyn, S. Kobsev, and M. Dubov, "Mode-Locking in 25-km Fibre Laser," ECOC 2010, 19–23, 2010.
10. V.I. Denisov, B.N. Nyushkov, and V.S. Pivtsov, "Self-mode-locked all-fibre erbium laser with a low repetition rate and high pulse energy," Quantum Electron. **40,** 25–27 (2010).
11. Y. Senoo, N. Nishizawa, Y. Sakakibara, K. Sumimura, E. Itoga, H. Kataura, and K. Itoh, "Ultralow-repetition-rate, high-energy, polarization-maintaining, Er-doped, ultrashort-pulse fiber laser using single-wall-carbon-nanotube saturable absorber," Opt. Express **18,** 20673–20680 (2010).
12. X. Li, X. Liu, X. Hu, L. Wang, H. Lu, Y. Wang, and W. Zhao, "Long-cavity passively mode-locked fiber ring laser with high-energy rectangular-shape pulses in anomalous dispersion regime," Opt. Lett. **35,** 3249–3251 (2010).
13. S. Kobtsev, S. Kukarin, S. Smirnov, S. Turitsyn, and A. Latkin, "Different generation regimes of mode-locked all-positive-dispersion all-fiber Yb laser," Proc. of SPIE, **7580,** 758028–2, (2010).
14. S.M. Kobtsev and S.V. Smirnov, "Fiber Lasers Mode-Locked Due to Nonlinear Polarization Evolution: Golden Mean of Cavity Length," Laser Phys. **21**(2), 272–276 (2011).

15. S. Smirnov, S. Kobtsev, S. Kukarin, and A. Ivanenko, "Three key regimes of single pulse generation per round trip of all-normal-dispersion fiber lasers mode-locked with nonlinear polarization rotation," Opt. Express **20**, 27447–27453 (2012).

16. N. Li, J. Xue, C. Ouyang, K. Wu, J.H. Wong, S. Aditya, and P.P. Shum, "Cavity-length optimization for high energy pulse generation in a long cavity passively mode-locked all-fiber ring laser," Appl. Optics **51,** 3726–3730 (2012).

17. A. Boucon, B. Barviau, J. Fatome, C. Finot, T. Sylvestre, M. W. Lee, P. Grelu, and G. Millot, "Noise-like pulses generated at high harmonics in a partially-mode-locked km-long Raman fiber laser," Appl. Phys. B, **7,** 1–5 (2012).

18. Z.Q. Luo, C.C. Ye, H.Y. Fu, H.H. Cheng, J.Z. Wang, and Z.P. Cai, "Raman fiber laser harmonically mode-locked by exploiting the intermodal beating of CW multimode pump source," Opt. Express **20,** 19905–19911 (2012).

19. T. Schreiber, B. Ortaç, J. Limpert, and A. Tünnermann, "On the study of pulse evolution in ultra-short pulse mode-locked fiber lasers by numerical simulations," Opt. Express **15,** 8252–8262 (2007).

20. F.W. Wise, A. Chong, and W.H. Renninger, "High-energy femtosecond fiber lasers based on pulse propagation at normal dispersion," Laser Photonics Rev. **2,** 58–73 (2008).

21. V.L. Kalashnikov, E. Podivilov, A. Chernykh, and A. Apolonski, "Chirped-pulse oscillators: theory and experiment," Appl. Phys. B **83**(4), 503–510 (2006).

22. P. Grelu and N. Akhmediev, "Dissipative solitons for mode-locked lasers," Nat. Photonics **6**(2), 84–92 (2012).

23. X. Liu, "Numerical and experimental investigation of dissipative solitons in passively mode-locked fiber lasers with large net-normal-dispersion and high nonlinearity," Opt. Express bf 17(25), 22401–22416 (2009).

24. A. Martinez and S. Yamashita, "Multi-gigahertz repetition rate passively modelocked fiber lasers using carbon nanotubes," Opt. Express **19,** 6155–6163 (2011)

25. O. Shtyrina, M. Fedoruk, S. Turitsyn, R. Herda, and O. Okhotnikov, J. Opt. Soc. Am. B **26,** 346 (2009).

26. S.K. Turitsyn, "Theory of energy evolution in laser resonators with saturated gain and non-saturated loss," Opt. Express **17,** 11898 (2009).

27. B.G. Bale, S. Boscolo, J.N. Kutz, and S.K. Turitsyn, "Intracavity dynamics in high-power mode-locked fiber lasers," Phys. Rev. A**81,** 033828 (2010).

28. S.K. Turitsyn, B. Bale, and M.P. Fedoruk, "Dispersion-managed solitons in fibre systems and lasers," Phys. Rep., **521**(4), 135–203 (2012).

29. B.G Bale, O.G. Okhotnikov, and S.K. Turitsyn, "Modeling and Technologies of Ultrafast Fiber Lasers" in *Fiber Lasers,* O. G. Okhotnikov, ed. (Wiley-VCH Verlag GmbH Co., 2012).

30. B. Oktem, C. Ülgüdür, and F. Ömer Ilday, "Soliton–similariton fibre laser," Nat. Photonics **4,** 307–311 (2010).

31. A.I. Chernykh and S.K. Turitsyn, "Soliton and collapse regimes of pulse generation in passively mode-locking laser systems," Opt. Lett. **20**(4), 398 (1995).

32. D. Tang, L. Zhao, and B. Zhao, "Soliton collapse and bunched noise-like pulse generation in a passively mode-locked fiber ring laser," Opt. Express **13,** 2289-2294 (2005).

33. D.S. Kharenko, O.V. Shtyrina, I.A. Yarutkina, E.V. Podivilov, M.P. Fedoruk, and S.A. Babin, "Highly chirped dissipative solitons as a one-parameter family of stable solutions of the cubic-quintic Ginzburg–Landau equation," J. Opt. Soc. Am. B **28**(10), 2314–2319 (2011).

1. Introduction

Cavity length is an important fiber laser system parameter that defines characteristics of generated optical pulses [1]. In the pulsed fiber lasers, a significant extension of the cavity length provides an opportunity to achieve substantial increase of the pulse energy [2, 3]. A number of theoretical studies and experimental demonstrations of high pulse energy fiber lasers with the cavity length of several kilometers without use of traditional techniques such as cavity dumping or Q-switching have been reported recently (it is difficult to cite all relevant papers on the subject, see e.g. [2–18] and references therein). Fiber lasers provide a possibility for use of a range of nonlinear mechanisms in building and shaping the radiation [20–33]. Nonlinear effects make numerical modelling of fiber lasers a challenging problem. The numerical modeling of fiber laser systems with ultra-long cavity length faces additional technical challenges such as a increased time of calculations and computational resources. Numerical modeling of lasers with such long resonators is also influenced by the impact of nonlinear effects leading to instabilities and stochastisation that requires a special attention in modeling. Recently, numerical modeling was applied to analyze properties of long fiber lasers passively mode-locked by the nonlinear polarization evolution with the cavity length from about 100 m [13–15] up to 8 km [3]. In this paper we focus on a scalar model of polarization-independent saturable absorber [19–29] and

present simulation results for pulse generation in fiber laser with long cavity length up to 2 km. Our goal here is to highlight impact on a modeling of initial field distribution (noise versus smooth small amplitude seeding field) and raise of modeling challenges with a growing cavity length.

2. Laser setup and mathematical model

Aiming at the analysis of the key physical effects rather than on a laser specifics, in this work we consider generic laser systems that can be well described by the scalar model [19–29].
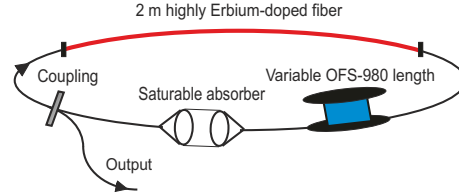

Fig. 1. The scheme of laser setup.

Figure 1 depicts the scheme of a fiber laser system considered in numerical modeling. The ring cavity consists of a 2m-long active Er-doped fiber, passive fiber of variable length, polarization-independent saturable absorber and an output coupler. Usually, in the cavities with the anomalous dispersion pulse propagation suffers from the soliton-like instabilities [29]. And the influence of nonlinear effects leading to the pulse breaking grows with the cavity length extension. The single-pulse regimes were obtained for 10 m cavity only using anomalous single-mode fiber SMF-28 as a passive fiber. The total cavity dispersion in this case was -0.0742 ps^2. That is why the fiber with the normal dispersion OFS-980 has been chosen for the numerical simulation.

Pulse evolution is modeled as a consecutive propagation through the fiber elements as shown in Fig. 1. Parameters of the laser system elements used in simulations are shown in the table 1. The laser operates at the central wavelength λ_0=1550 nm.

The round trip in such systems is $T_R = n_0 \cdot L/c$ where $L = L_{AF} + L_{PF}$ is a total cavity length, L_{PF} is a passive fiber length, c is a speed of light and the refractive index of the core $n_0 \approx 1.5$. Propagation of radiation in an active fibre is governed by the generalized nonlinear Schrödinger equation (NLSE) with the input field $A(t, z = 0) = A_{in}(t)$ (that is determined by the previous round trip, apart from the very first round trip when it is an initial seeding distribution):

$$\frac{\partial A}{\partial z} = -i\frac{\beta_2}{2}\frac{\partial^2 A}{\partial t^2} + \frac{\beta_3}{6}\frac{\partial^3 A}{\partial t^3} + i\gamma|A|^2 A + \widehat{g}A - \alpha A. \tag{1}$$

When simulating active fiber in mode-locked lasers, gain saturation and gain spectral dependence (an effective gain filtering) have to be taken into account. The effect of the gain spectral dependence in the operator $\widehat{g}$ is typically introduced in the frequency domain using Lorentzian line-shape justified by the predominantly homogenous broadening mechanism in rare doped glasses:

$$g(\omega) = \frac{1}{1 + \frac{E}{E_{satG}}} \times \frac{g_0}{1 + \left(\frac{\omega - \omega_0}{\Omega_g}\right)^2}. \tag{2}$$

Here $\omega_0 = 2\pi c/\lambda_0$ is the central frequency of the gain and $\Omega_g = \frac{2\pi c}{\lambda_0^2}\Lambda_g$ is the gain bandwidth (given either in frequency Ω_g or wavelength Λ_g). The gain is saturated with the growth of

Table 1. Values of fiber laser parameters.

Element	Parameter	Value
Active Er-doped fibre [30]	Length L_{AF}	2 m
	2nd order dispersion β_2	76.9 fs^2/mm
	3d order dispersion β_3	168 fs^3/mm
	Nonlinear parameter γ	0.00932 1/W/m
	Gain bandwidth Λ_g	50 nm
	Small signal gain g_0	5.4 dB/m
	Saturation power P_{satG}	20 mW
Passive fibre OFS-980 [30]	2nd order dispersion β_2	4.5 fs^2/mm
	3d order dispersion β_3	109 fs^3/mm
	Nonlinear parameter γ	0.0021 1/W/m
	Fiber losses α	0.2 dB/km
Saturable absorber [29]	Modulation depth q_0	10%
	Saturation power P_{sat}	3.69 W
Out-coupler	Out-coupling parameter R_{out}	Variable around 90%

the total pulse energy $E = \int |A|^2 dt$, here $E_{satG} = P_{satG} \times T_R$. In this paper we consider regime when the change of the total cavity length and corresponding additional losses are compensated mostly by adjustment of the out-coupling. The amplifier small gain $G_0 = g_0 L_{AF}$ is kept constant, however the total gain varies through gain saturation (due to increasing pulse energy in a longer cavity).

The passive fiber has been simulated using the standard generalized NLSE equation:

$$\frac{\partial A}{\partial z} = -i\frac{\beta_2}{2}\frac{\partial^2 A}{\partial t^2} + \frac{\beta_3}{6}\frac{\partial^3 A}{\partial t^3} + i\gamma|A|^2 A - \alpha A. \tag{3}$$

The NLSE has been solved using the symmetric split-step Fourier method for both active and passive fiber.

We consider evolution of electric field in saturable absorber with the parameters presented in Table 1 suitable for saturable absorber with high saturation power. The saturable absorber is described by a simplified transfer function $T(t) = [1 - q(t, P_{in}(t))]$ where $P_{in}(t) = |A_{in}(t)|^2$ and q can be found from the equation:

$$q(t) = \frac{q_0}{1 + \frac{|A_{in}(t)|^2}{P_{sat}}}. \tag{4}$$

By solving this equation we determine q as a function of time and the input field. The output coupler is described by $A_{out} = R_{out}A_{in}$ and $A_{cavity} = (1 - R_{out})A_{in}$ where A_{in} is the field before out-coupler, A_{out} is the fraction of the total field leaving cavity and A_{cavity} is the part that is left in the ring resonator.

3. Modeling results

The first goal of our work is to evaluate and demonstrate importance of an initial "seeding" field distribution in modeling of pulse generation in such long cavity lasers. Small amplitude smooth initial seeding pulse (e.g. having Gaussian shape) is routinely used for modeling of mode-locking lasers. This is based on assumption that the asymptotic state generated after many round

trips should not depend on any features of the initial noise. Typically this is not a problem and initial conditions do not play significant role in determination of a final asymptotic state in the nonlinear dissipative system such as laser. However, in the case of increased cavity length laser pulses with noisy internal structure (double scale solution) are observed [4]. This indicates a potential importance of the properties of a seeding distribution (smooth functions versus noise). The final attractors can be different for smooth initial field and noise-based seeding as we will demonstrate below. In this work we perform a comparison of pulses generated from smooth initial seed versus pulses generated from initial noise. We use white noise distributions as an initial field (apart from numerical runs with smooth seeds for comparison purposes). The grid consists of 2^{14} points in time domain and 4000 nodes in space at the cavity round-trip. The time domain modeling window was about 18 ns. It took approximately 48 hours to calculate 2000 cavity round-trips with the round-trip time being $T_R = n_0 \cdot L/c \approx 0.1 \mu s$ for 2 km cavity length.

We observe that resulting attractors do depend on the initial conditions. For instance, single-pulse regime obtained from initial smooth field distribution is not necessarily the same as the regime found for a white noise initial distribution of the same power. The basin of attraction for each such asymptotic state is different and this tendency is getting stronger with the increase of the cavity length. Therefore, numerical modeling of long cavity lasers should take this effect into account. In Fig. 2 we show two examples of the generated pulses: in Fig. 2(a) an initial condition is a Gaussian pulse with an average power (the pulse energy divided by the modeling time interval) of 0.7 mW and in the Fig. 2(b) the initial condition was a white noise with the same average power of 0.7 mW. Figure 2(c) shows the attractors' dependence on the initial conditions. The blue line corresponds to the evolution of the Gaussian initial field distribution and the green line - of the white noise to the attractors marked with the circles. Here root-mean-square (RMS) pulse characteristics are defined in a standard manner:

$$P_{RMS} = \frac{\int |A|^4 dt}{E}; \quad T_{RMS}^2 = \frac{\int t^2 |A|^2 dt}{E}, \quad (5)$$

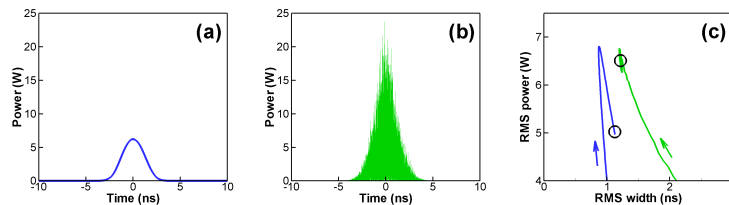where P_{RMS} and T_{RMS} are RMS power and RMS pulse width respectively.

Fig. 2. Resulting pulses in case of: a) Gaussian initial field distribution; b) White noise initial distribution. Here $L = 2$ km, average power of the initial pulse – 0.7 mW. c) Attractors for different initial distributions: the blue line shows the evolution of the Gaussian initial field distribution and the green line – of the white noise to the attractors marked with the circles.

To define generation of a single pulse, we applied the following convergence procedure. The regime is accepted to be stable when the relative variation ε of pulse energy $\varepsilon = |E_i - E_{i+1}|/E_i$ does not exceed 10^{-3}, and, additionally, the relative variations of pulse width and spectral power do not exceed 10^{-2} and 10^{-2}, respectively, during at least 200 round trips. In this case simulations were stopped and the generated pulse was considered as a stable asymptotic state. We have found that in the case of relatively short cavity lengths (up to 32 m) the same single-pulse stable regimes can been obtained from rather different self-starting regimes. The pulse energy stabilization for cavity length of 32 m has been achieved after more than 4000 round−trips. For

shorter cavities it took approximately 1000 round trips to approach the steady state in terms of the energy evolution. However, for ≥ 42 m cavity lengths the stable pulse regimes as defined above might not be reached even after 120000 round-trips. Figure 3 presents the dependence of the approximate number of cavity round trips, required to achieve the stable single pulse regime, on the cavity length. It is seen that there is an exponential growth of a required round trips number for cavities longer than 20 m.
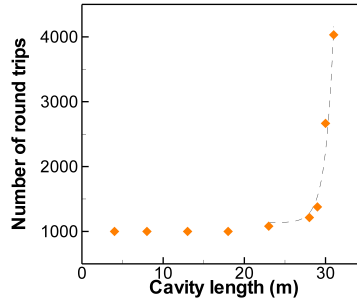
Fig. 3. The dependence of the approximate number of cavity round trips, necessary to obtain the energy steady state, on the cavity length. Dashed line shows the exponential dependence of round trips number for cavities longer than 20 m.

The black line in the Fig. 4(a) shows the resulting pulse shape and spectrum shape (in the inset) for the 32 m cavity. The generated pulse has a smooth bell-type temporal shape. As one can see from the inset in Fig. 4(a), the pulse spectrum has the typical form (characteristic for highly-chirped pulses) with the sharp drops at the edges [20].

The black line in the Fig. 4(b) presents the generated pulse after 2000 round-trips for 2002 m cavity length. It was not possible in our modeling to get a smooth pulse shape even after 20000 round-trips. The typical result shows an envelope with a ns scale width and strong noisy oscillation components inside the envelope [4]. The noisy content can be linked to the pulse collapse regimes studied in [31,32]. In this case let us consider such a regime to be "stabilized" when the relative variation ε of pulse energy $\varepsilon = |E_i - E_{i+1}|/E_i$ does not exceed 10^{-3}. The resulting output pulse energy are 0.5 nJ and 16 nJ for a cavity length of 32 m and 2002 m, respectively.

The insets in the Fig. 4 show the averaged pulse spectra for pulses generated from the initial noise. In the case of 2002 m cavity length the spectrum was averaged over 10 round-trips. As one can see, different amplification for 32 m and 2002 m cavity can be described by the different spectral characteristics.

The red lines in Figs. 4(a) and (b) show for comparison the Gaussian pulse fit with the same RMS characteristics as the generated pulses defined in a standard manner as follows: for a Gaussian pulse $\sqrt{P} \exp(-t^2/\tau^2)$, the corresponding RMS parameters are: $P = \sqrt{2}P_{RMS}$ and $\tau^2 = 4 \cdot T_{RMS}^2$.

Figure 5 shows the intra-cavity dynamics of energy and RMS characteristics (width and power) for a pulse obtained from the initial white noise for different cavity lengths. One can see rather different dynamics of the RMS pulse width for short and long laser cavity. In the case of long cavity a RMS pulse width is slightly compressed in the gain medium. Overall, the relative RMS pulse width variation is not large in both cases.

The pulse is amplified inside the active fiber and the behavior of the RMS width during the pulse propagation through the active fiber depends on the total cavity length; passive fiber stretches pulse and slightly decreases its power; saturable absorber decreases RMS width and
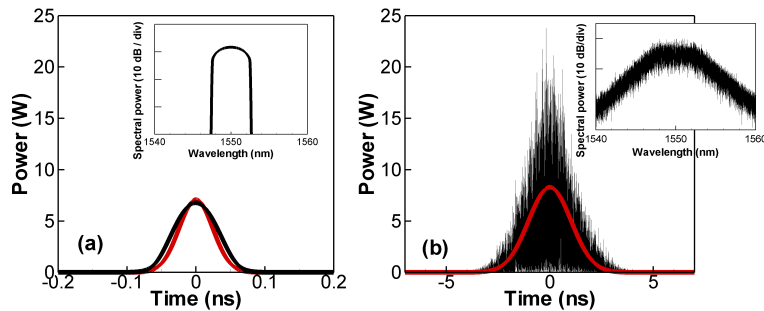
Fig. 4. Black line – pulses generated from the white noise as the initial distribution, red line – the Gaussian pulse fit with RMS characteristics in case of: a) 32 m cavity length; b) 2002 m cavity length. Insets show the corresponding averaged spectra of pulses generated from the noise.

insignificantly reduces RMS power; an output coupler decreases pulse power. The visual difference of the RMS pulse width dynamics in the active fiber between two regimes is attributed to the definition of RMS characteristic and can be explained by the significant growth of the energy in case of long resonator compared to the 32 m cavity. As a matter of fact there is a pulse broadening in active fiber for both long and short cavities. There is no chirp-free point inside the cavity as it is typical for the lasers with all-normal dispersion configurations [20]. In the lasers with longer cavity the intra-cavity dynamics is substantially changed [15].

During the pulse propagation in the saturable absorber, not only the modulation depth affects the energy losses, but also the ratio of pulse power and the saturation power. So in fact, the real saturable absorber losses are smaller than 10% (the real losses are 4% for 32 m and 2 km cavity). That is a reason of insignificant influence of the saturable absorber on the pulse energy. If a higher modulation depth is used, the pulses would have a lower energy and shorter duration. This decrease of the energy mainly caused by the more significant pulse compression comparing to the decrease of the peak power. For the 32 m cavity the pulse energy decreases from 0.58 nJ to 0.54 nJ with the increasing of the modulation depth from 10% to 13% (the saturation power was constant). In this case the real losses amount to 5%.

Figures 6 (a) and (b) show three-dimensional picture of an intra-cavity temporal pulse shape evolution and dynamics of the spectrum of a single-pulse stable regime in cavities having 32 m length and 2002 m respectively. The evolution is quite typical for lasers with all-normal cavity dispersion [20].

Finally we present results of numerical analysis of the impact of a varying cavity length (using out-coupling parameter R_{out} to adjust energy balance, while keeping small signal gain $g_0 \cdot L_{AF}$ constant) on the generated pulse energy. In general, cavity extension leads to increase of a pulse energy and saturation of the amplifier gain. This is compensated by adjustment of the out-coupling coefficient and increased cavity losses [26]. In other words, the total cavity losses $(R_{in} + \alpha \cdot L_{PF})$ (in dB), where $R_{in}(dB) = 10 \cdot \ln(1 - R_{out})/\ln 10$ and L_{PF} – passive fiber length are affected by the the cavity extension, but first of all through gain saturation and out-coupling adjustment rather than through additional losses of a passive fiber. As one can see from Fig. 7, the character of the output energy dependence on the cavity length is different for small and long resonator lengths. The energy depends linearly on the cavity length for small resonators. However, this growth is saturated at larger length because of the change of the relation between the gain and losses. Dashed line on Fig. 7 depicts the fit of the energy dependence on the cavity
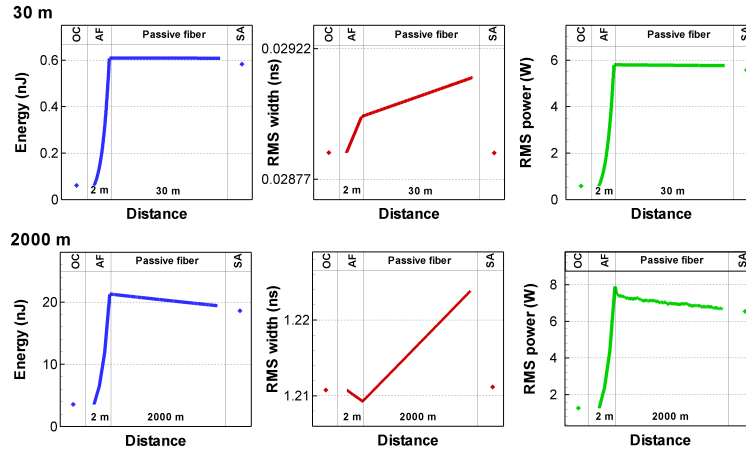
Fig. 5. The intra-cavity dynamics of energy and RMS characteristics of pulse obtained from the initial white noise for different cavity lengths. Here OC is output coupler, AF – active fiber and SA – saturable absorber.
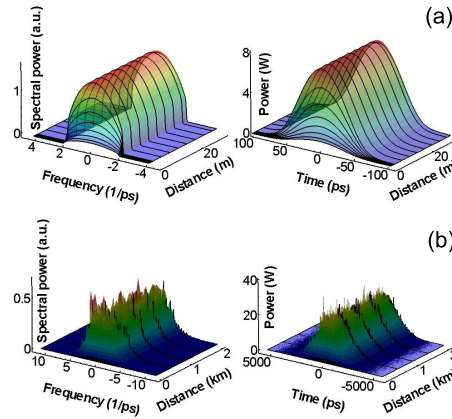

Fig. 6. The intra-cavity spectrum and temporal pulse shape evolution in: a) 32 m cavity; b) 2002 m cavity.

length, gain and losses. This line is the following fitting formula (compare to [26]):

$$E = a \cdot L \frac{g_0 \cdot L_{AF} - (R_{in} + \alpha \cdot L_{PF})}{R_{in} + \alpha \cdot L_{PF}}, \tag{6}$$

where a is some fitting constant factor.

Stable (as defined above) single pulsed regimes have not been found for cavity lengths exceeding 2002 m. Figure 8 depicts the output pulse RMS characteristics' dependence on the length of the cavity. The intervals illustrate the variance (over five realizations) of the results due to different realizations of the initial white noise distributions.

We have observed a significant spectral broadening of the pulse for relatively short cavity lengths, while the pulse spectrum width stabilizes after the cavity length of approximately 200 m. This can be result of the considered 50 nm gain bandwidth. Since the spectral width Δ is connected with the RMS power in the following way: $\Delta = \sqrt{\gamma P_{RMS}/\beta}$, where γ and β are
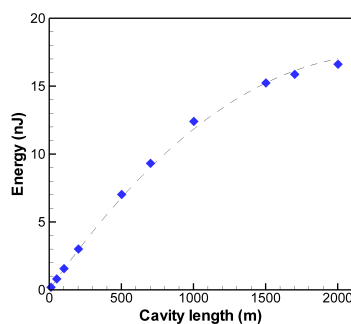
Fig. 7. Output energy dynamics with the cavity length extension for the white noise as an initial distribution. Dashed line is a fit of the following expression: $E = a \cdot L \frac{g_0 \cdot L_{AF} - (R_{in} + \alpha \cdot L_{PF})}{R_{in} + \alpha \cdot L_{PF}}$.
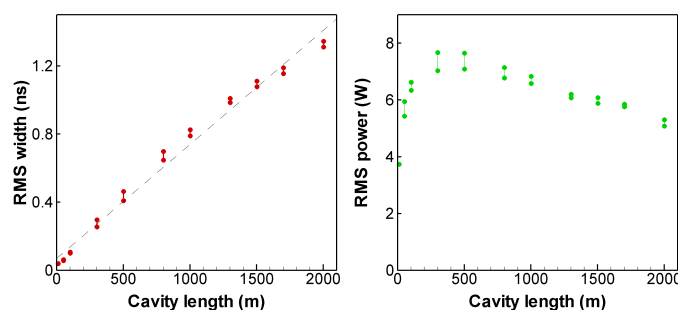

Fig. 8. Dynamics of RMS characteristics with a cavity length extension for white noise as an initial distribution.

cumulative nonlinearity and dispersion respectively [33], one can see the RMS power dynamics presented on the Fig. 8.

4. Conclusion

In this paper we presented the modeling results of the ring cavity passively mode locked fiber laser with the total cavity length up to 2002 m. We have shown that in fiber lasers with the long and ultra-long cavities impact of an initial noise should be taken into account. Use of a smooth initial field distributions can lead to very different asymptotic attractor. We have studied lasing regimes when the increased cavity length leads to increases pulse energy and resulting gain saturation (under condition of a constant small gain). In this case the energy balance adjustment is done via varying out-coupling parameters. We presented an approximate formula describing energy dependence on a cavity length for a considered regime of single pulse generation in long cavity fiber lasers.

Acknowledgment